Rapid Communications | Editors' Suggestion

Tunneling anisotropic magnetoresistance via molecular π orbitals of Pb dimers

Johannes Schöneberg,[1] Paolo Ferriani,[2] Stefan Heinze,[2] Alexander Weismann,[1] and Richard Berndt[1]
[1]*Institut für Experimentelle und Angewandte Physik, Christian-Albrechts-Universität zu Kiel, 24098 Kiel, Germany*
[2]*Institut für Theoretische und Astrophysik, Christian-Albrechts-Universität zu Kiel, 24098 Kiel, Germany*

(Received 6 October 2017; revised manuscript received 22 December 2017; published 22 January 2018)

Pb dimers on a ferromagnetic surface are shown to exhibit large tunneling anisotropic magnetoresistance (TAMR) due to molecular π orbitals. Dimers oriented differently with respect to the magnetization directions of a ferromagnetic Fe double layer on W(110) were made with a scanning tunneling microscope. Depending on the dimer orientations, TAMR is absent or as large as 20% at the Fermi level. General arguments and first-principles calculations show that mixing of molecular orbitals due to spin-orbit coupling, which leads to TAMR, is maximal when the magnetization is oriented parallel to the dimer axis.

DOI: 10.1103/PhysRevB.97.041114

Spin-orbit coupling (SOC) links spin and momentum degrees of freedom by the Hamiltonian $H_{\mathrm{SOC}} = \xi \mathbf{LS}$ where ξ is the SOC constant and $\mathbf{L}$ and $\mathbf{S}$ are the orbital momentum and spin operators, respectively. It is the origin of phenomena, such as magnetocrystalline anisotropy and anisotropic magnetoresistance which are of fundamental interest and important for applications. Studies of the magnetocrystalline anisotropy at the single atom level have highlighted the effect of the environment of an atom on SOC [1–5]. For example, the spin lifetime is significantly longer in FeCu dimers on Cu_2N than in single Fe atoms [3]. Similarly, spin excitations are affected by the adsorption site and nearby atoms [6–8]. Anisotropic magnetoresistance (AMR), the relative change in resistivity as a function of magnetic-field orientation, is a rather small effect in elemental bulk ferromagnets [9] but can be enhanced in bulk alloys [10] or in tunneling devices [11–15] to values of some 10%. Atomic scale investigations of AMR with a scanning tunneling microscope (STM) have so far only been reported for isolated Co and Ir adatoms [14,16].

To tune SOC at a single atom, the high rotational symmetry of the atom should be reduced. Here, this is achieved by constructing dimers from single Pb atoms on an Fe double layer substrate that exhibits in-plane and out-of plane magnetizations in magnetic domains and domain walls, respectively [17]. Pb exhibits a strong spin-orbit interaction due to its large atomic number Z. Assuming the bare Coulomb potential and atomic wave functions the strength of SOC scales with the principal and orbital quantum numbers n and l as $\xi \propto Z^4 n^{-3} l^{-2}$. Accordingly, the $6p$ states of Pb should have a larger SOC constant than all $3d$ or $5d$ states studied so far [14,16,18]. This is supported by first-principles calculations for FePt alloys [19] which reported values of $\xi_{6p}^{\mathrm{Pt}} = 2.217$ and $\xi_{5d}^{\mathrm{Pt}} = 0.571$ eV for the $6p$ and $5d$ Pt states, respectively. Experimentally, we indeed find a tunneling anisotropic magnetoresistance ratio (TAMR) exceeding 20% in suitably oriented Pb dimers.

The idea motivating our experiment may be understood by considering a Pb dimer which interacts only weakly with the surface. The dimer axis (assumed to be y) defines the orientation of the molecular orbitals (MOs). The tunneling current is dominated by the π_z molecular orbitals as they extend farthest into the vacuum. If the magnetization direction is along the dimer axis the π_x and π_z molecular orbitals can mix via SOC, which reduces the vacuum local-density of states (LDOS). For a spin-quantization axis perpendicular to the dimer axis, SOC would mix π and antibonding σ^* molecular orbitals which are further separated in energy than π_x and π_z orbitals, resulting in a smaller SOC-induced modification of the LDOS. These variations of the LDOS under rotation of the spin-quantization axis lead to the TAMR [17]. Consequently, spin-quantization axes parallel and perpendicular to the y direction will show maximal and minimal SOC-induced mixings, respectively, which lead to maximal TAMR.

To experimentally test this concept, we performed scanning tunneling spectroscopy in ultrahigh vacuum at 4.4 K. W(110) surfaces were cleaned by repeated heating in an O_2 atmosphere and brief annealing at 2200 K. Fe double layers were grown by sublimation from an Fe-covered filament onto the W crystal held at 500 K. Pb atoms were evaporated on the cold surface from a Pb-coated W filament. These atoms were moved at a resistance of 25 kΩ (100 mV, 4 μA) to build dimers with different orientations [Figs. 1(a) and 1(b)]. Atomically resolved constant-current topographs [Fig. 1(c)] provide information on the adsorption geometries of the dimers. Assuming that Pb atoms adsorb at hollow sites of the Fe surface the dimers are oriented along the [001] and [1$\bar{1}$1] directions, respectively [Figs. 1(d) and 1(e)]. We were unable to construct [1$\bar{1}$0]-oriented dimers, whose axes would be perpendicular to the magnetizations of both domains and domain walls. However, [1$\bar{1}$1] dimers are rotated by 55° with respect to the in-plane magnetization on domain walls, whereas the magnetization is collinear with the [001] dimer. On domains, the magnetization is perpendicular to the surface and both dimer types.

Figures 2(a) and 2(b) display six dimers adsorbed on a domain or a domain wall. dI/dV spectra were acquired with a W tip [20]. The apparent heights of the dimers are identical on domains and domain walls at a sample voltage of $V \approx 1$ V, which was therefore used to adjust the tip-sample distance prior to spectroscopy. At positive V the spectra are hardly affected by the magnetization direction with all dimers showing an unoccupied state at ≈600 mV. The [001] dimer exhibits an

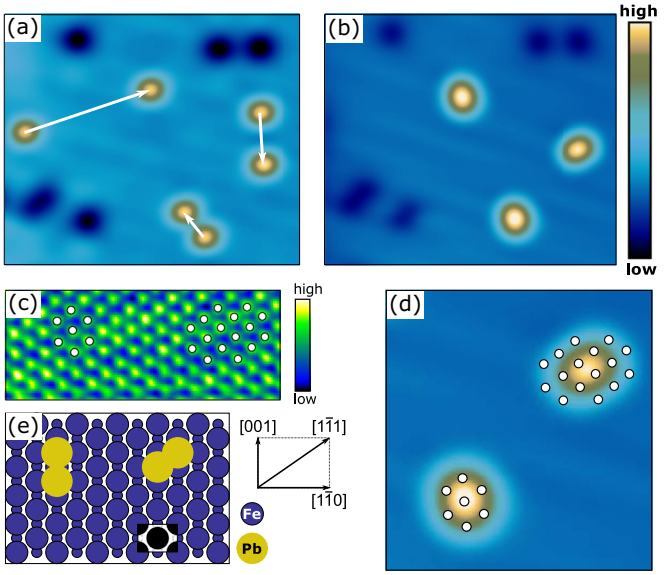

FIG. 1. (a) Constant-current topograph of six single Pb atoms (protrusions) on double-layer Fe on W(110) (6.6 × 9 nm^2, 100 mV). Depressions are due to defects. Pb atoms were manipulated with the STM tip at a resistance of 25 kΩ (100 mV, 4 μA) as indicated by the arrows. (b) Dimers with two orientations were obtained (7 × 9 nm^2, 1 V). (c) Atomically resolved topograph of the substrate lattice (4.7 × 1.9 nm^2, 70 mV, 5 μA). (d) Substrate lattice superimposed onto dimers assuming adsorption to hollow sites (3.8 × 4 nm^2, 1 V). (e) Resulting geometries of dimers oriented along the [001] and ([1$\bar{1}$1]) directions.

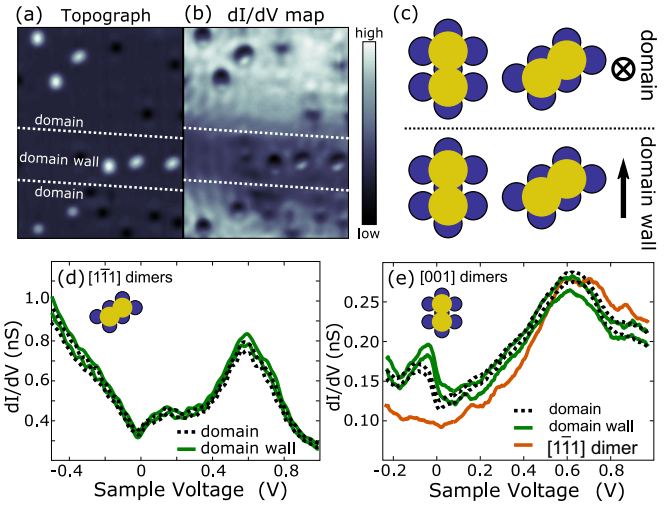

FIG. 2. (a) Topograph and (b) simultaneously recorded dI/dV map of six dimers (13 × 19 nm^2, 70 mV). The upper (lower) three dimers are adsorbed on a domain (domain wall) with an out-of-plane (in-plane) magnetization. (c) This leads to four angular configurations of spin quantization and coordination axes. (d) Averaged dI/dV spectra of [1$\bar{1}$1] dimers on a domain (the dotted curves) and a domain wall (the solid curves) (feedback opened at 1 V, 500 pA) are similar. (e) Spectra of [001] dimers show significant differences at $V < 0$ V. The spread between curves with the same style indicates uncertainties (standard deviation of the averaged data). Different tips were used in (d) and (e). A [1$\bar{1}$1]-dimer spectrum (the orange curve) is shown for comparison. Modification of the tip affects the spectra. However, the characteristics discussed here were present in all spectra.

additional occupied state at −50 mV which is absent on [1$\bar{1}$1] dimers as illustrated by the dI/dV data in Fig. 2(e). This peak is significantly affected by the magnetization direction, whereas the dI/dV spectra of the [1$\bar{1}$1] dimer remain essentially unchanged. At first glance this is in agreement with the conclusion of the simplified model: Only for the [001] dimer the magnetization vector is collinear with the coordination direction.

The influence of the magnetization direction on the peak at −50 mV becomes clearer in Fig. 3(a) displaying dI/dV spectra measured on [001] dimers over a narrower energy interval around the Fermi energy E_F. Their difference is quantified by the TAMR $= (dI_\perp/dV - dI_\parallel/dV)/(dI_\perp/dV)$, where $I_\perp$ ($I_\parallel$) denotes the current for a Pb dimer on a domain (domain wall). As shown in Fig. 3(b) the TAMR reaches its maximal value of $-(23 \pm 3)$% at $V = -14$ mV [21]. At E_F, the TAMR is $-(21 \pm 5)$%, which is twice as large as values reported of single Co adatoms [14]. In addition, the dI/dV peak shifts by 21 mV with the magnetization direction and exhibits a TAMR of ≈ -14% [the gray areas in Figs. 3(a) and 3(b)].

The relationship between the dimer states and those of the Fe substrate is further characterized by spin-polarized dI/dV spectra. For recording these data, the tip was covered with Fe and further modified until a spin contrast between domains was achieved, thus ensuring an out-of-plane sensitivity of the tip [22]. Figure 3(c) shows data from [001] dimers on Fe domains with opposite magnetizations. The resulting conductance asymmetries [Fig. 3(d)] are positive at the peak positions. Consequently, the dimer state at −50 mV has the same spin character as the minority d_{z^2} Fe state [17] albeit with lower spin polarization. The similar energies of the Fe and the dimer states, their similar shifts with the magnetization direction, and

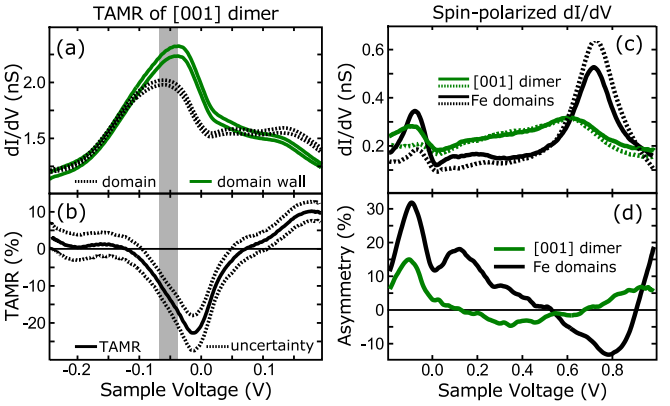

FIG. 3. (a) Detailed [001]-dimer spectra. (b) TAMR of the spectra in (a). The dashed curves represent uncertainty margins. The gray areas mark the peak positions of the dI/dV spectra. (c) Spin-polarized dI/dV spectra of [001] dimers and Fe domains. The dashed and solid curves correspond to oppositely polarized domains and dimers adsorbed on them. (d) Asymmetry of the spectra in (c) defined by $(dI_\alpha/dV - dI_\beta/dV)/(dI_\alpha/dV + dI_\beta/dV)$ where α and β denote the spectra of oppositely polarized domains.

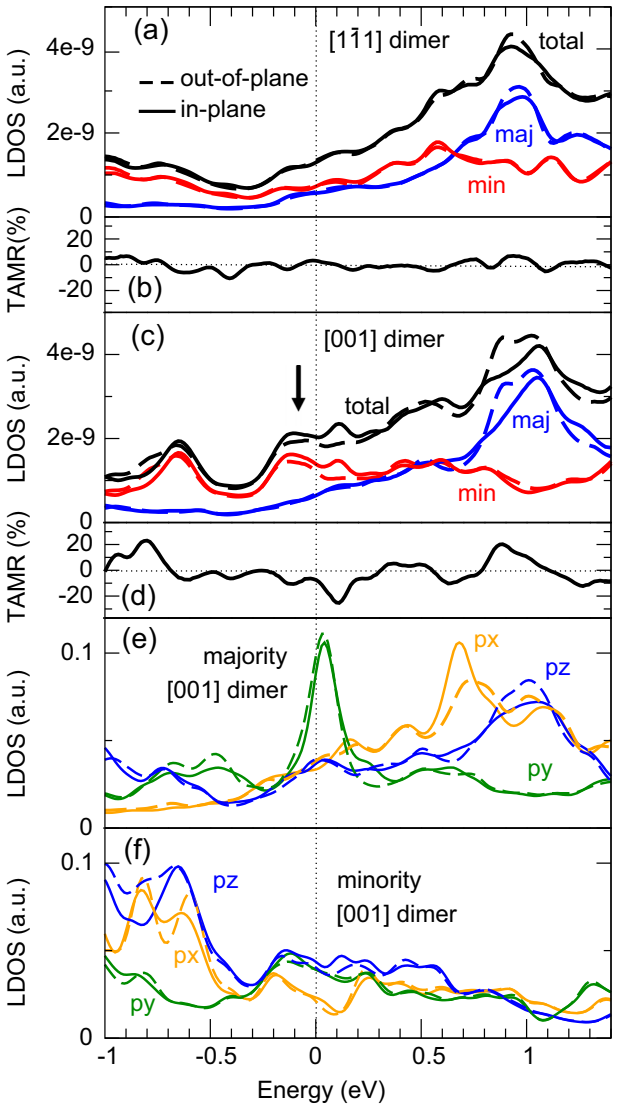

FIG. 4. (a) Total and spin-resolved vacuum LDOS 6.8 Å above a [1$\bar{1}$1] dimer on Fe/W(110) for out-of-plane (the dashed curve) and in-plane (the solid curve) magnetizations. (b) TAMR obtained from the LDOS. (c) and (d) LDOS and TAMR for the [001] dimer as in (a) and (b). (e) and (f) Orbital decomposition of the LDOS of the [001] dimer for majority and minority channels. The blue, green, and gold colors indicate p_z, p_y, and p_x orbitals at the Pb atoms. The solid and dashed curves denote in-plane and out-of-plane magnetizations, respectively.

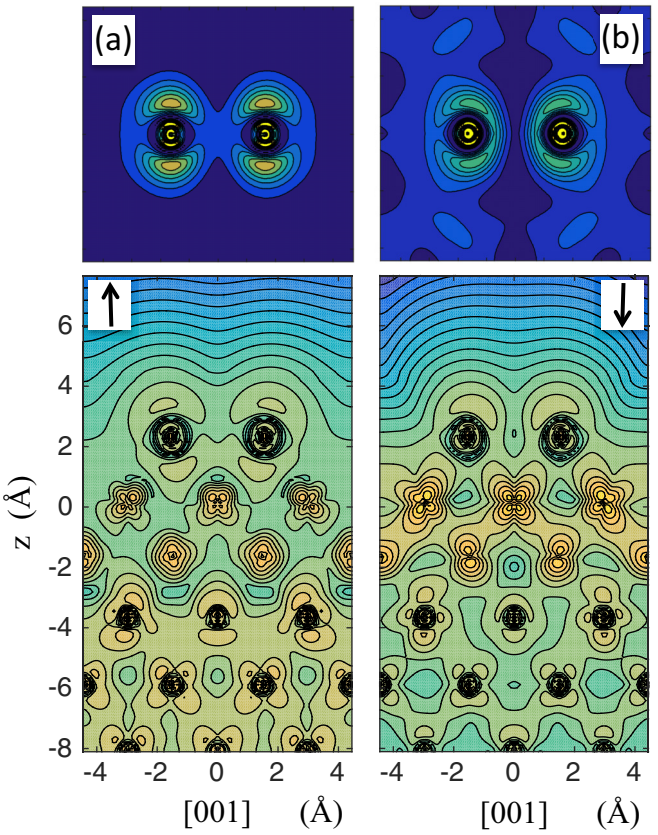

FIG. 5. Spin-resolved charge-density maps of the [001] dimer. The upper panels show a cross-sectional plot through the Pb dimers parallel to the surface, whereas the lower panels show a cross section through the dimers perpendicular to the film. The top Fe layer defines zero on the z axis. The Pb dimer atoms are located $\approx$2 Å above the Fe layer. (a) Majority density in the energy interval $[E_F + 0.85, E_F + 0.95$ eV]. (b) Minority density in the range of $[E_F - 0.2, E_F - 0.1$ eV]. Majority and minority refer to the spin directions of the Fe film.

their identical spin characters strongly suggest that they are related.

We performed first-principles calculations based on density functional theory for a model system comprising a symmetric film of five W(110) layers, two Fe(110) layers, and two Pb atoms on each side of the film. A c(4 × 6) surface unit cell with 12 W atoms per layer was used. The in-plane lattice constant of W(110) was fixed to the experimental value of 316.5 pm. The structure was relaxed using the projected augmented-wave method [23,24] in the generalized gradient approximation (Perdew-Burke-Ernzerhof functional [25]) employing four k points in the irreducible part of the two-dimensional Brillouin zone until the forces were below 0.015 eV/Å. To analyze the electronic structure we applied the full-potential linearized augmented plane-wave method in the local-density approximation [26] as implemented in the FLEUR code [27]. Spin-orbit coupling was included self-consistently as described in Ref. [28]. A plane-wave cutoff of 3.9 a.u.$^{-1}$ and 196 $k_\parallel$ points were used to calculate the LDOS.

Structural relaxation leads to a Pb distance of 3.3 Å in both dimers, a value of $\approx$10% larger than for free Pb dimers [29]. The axis of the [1$\bar{1}$1] dimer deviates by 58.7° from the [001] direction, which is slightly larger than in the unrelaxed geometry (Pb atoms at hollow sites). In both dimers the Pb atoms carry a small induced spin moment of $\approx 0.09\mu_B$. The orbital moment changes with the magnetization direction. For an out-of-plane magnetization (dimers on the domains), the orbital moment is similar for both dimers ($m_l^{\perp} \approx 0.008\mu_B$). For an in-plane magnetization along the [001] direction, however, we find a much larger orbital moment for the [001] dimer than for the [1$\bar{1}$1] dimer ($m_l^{[001]} \approx 0.009\mu_B$ vs $0.005\mu_B$) in line with the general symmetry arguments.

To compare with the experimental dI/dV spectra we calculated the LDOS in vacuum for both dimers. The LDOS of both dimers exhibits a pronounced peak between 0.9 and 1 eV

above E_F, which has a majority spin character with respect to the Fe substrate [Figs. 4(a) and 4(c)]. At the Pb atoms it has p_z symmetry [Fig. 4(e)] and forms a molecular π_z state [Fig. 5(a)] [30]. This state hybridizes only weakly with the Fe states because the majority d states are fully occupied leading to nearly perfect p_z lobes [Fig. 5(a)]. Therefore, the state is rather independent of the dimer orientation. We attribute the peak at $\approx$0.6 V in the experimental spectra of both dimers to this unoccupied state.

In agreement with the experiments, only the [001] dimer exhibits a minority-spin-related peak just below E_F [Fig. 4(c)]. It has p_z symmetry at the Pb atoms [Fig. 4(f)] and, as suggested by the experimental data, it hybridizes strongly with the d_{z^2} states of the Fe layer. The axis of the p_z orbitals at the Pb atoms are tilted towards the Fe atoms underneath due to the overlap with the tilted d_{z^2} states [Fig. 5(b)]. This leads to a canting of the upward pointing p_z lobes towards the center of the dimer [Fig. 5(b)]. The downward pointing lobes of the p_z orbitals, on the other hand, are not discernible due to the strong hybridization with the Fe d_{z^2} states. This hybridization is suppressed for the [1$\bar{1}$1] dimer due to its misalignment with the lattice of the underlying Fe layer.

Whereas the LDOS of the [001] dimer shows clear differences between in-plane and out-of-plane magnetizations, the difference is small for the [1$\bar{1}$1] dimer. This is reflected by the TAMR, which reaches $\approx$20% in the former case and is virtually absent in the latter case [Figs. 4(b) and 4(d)]. For the [001] dimer, the TAMR below E_F matches the experimental results in sign and order of magnitude. It is caused by a shift and reduced height of the peak at ≈ -0.12 eV [arrow in Fig. 4(c)], similar to the observation in dI/dV spectra [cf. Fig. 3(a)]. The different LDOS for in-plane magnetization results from SOC, which mixes p_x and p_z orbitals with the same spins [Figs. 4(e) and 4(f)]. As seen in Fig. 5(b) these hybrid Pb-Fe interface states are of π_x and π_z molecular-orbital character at the dimer. In contrast, the p_y states lead to σ-type MOs, which do not change much between domains and domain walls. In the [1$\bar{1}$1] dimer the magnetization is rotated with respect to the dimer axis, and the spin-orbit matrix element is reduced, leading to small mixing and TAMR, in agreement with the experiments. More precisely, $\langle \pi_z, \downarrow | H_{\mathrm{SOC}} | \pi_x, \downarrow \rangle \propto \cos\phi \sin\theta$, where $\downarrow$ is the minority-spin direction and ϕ and θ are the angles between the magnetization and the dimer axis y and the surface normal z, respectively. This mixing of the orbitals results in a change in the LDOS which scales as the square of the matrix element [17,31] and amounts to a reduction of the TAMR for the [1$\bar{1}$1] dimer by a factor of about 4 with respect to the [001] dimer [cf. Figs. 4(b) and 4(d)].

In conclusion, Pb dimers on a ferromagnetic substrate exhibit TAMR as large as 20% close to the Fermi level. It is due to spin-orbit-induced mixing of molecular π orbitals and crucially depends on the orientation of the magnetization with respect to the dimer axis. First-principles calculations show that its origin is a π_z orbital of the Pb dimer which strongly hybridizes with the underlying Fe layers.

Financial support by Deutsche Forschungsgemeinschaft through SFBs 668 and 677 as well as computational resources provided by the HLRN are gratefully acknowledged.

[1] P. Gambardella, S. Rusponi, M. Veronese, S. S. Dhesi, C. Grazioli, A. Dallmeyer, I. Cabria, R. Zeller, P. H. Dederichs, K. Kern, C. Carbone, and H. Brune, Science **300**, 1130 (2003).

[2] C. F. Hirjibehedin, C.-Y. Lin, A. F. Otte, M. Ternes, C. P. Lutz, B. A. Jones, and A. J. Heinrich, Science **317**, 1199 (2007).

[3] S. Loth, M. Etzkorn, C. P. Lutz, D. M. Eigler, and A. J. Heinrich, Science **329**, 1628 (2010).

[4] A. A. Khajetoorians, S. Lounis, B. Chilian, A. T. Costa, L. Zhou, D. L. Mills, J. Wiebe, and R. Wiesendanger, Phys. Rev. Lett. **106**, 037205 (2011).

[5] I. G. Rau, S. Baumann, S. Rusponi, F. Donati, S. Stepanow, L. Gragnaniello, J. Dreiser, C. Piamonteze, F. Nolting, S. Gangopadhyay, O. R. Albertini, R. M. Macfarlane, C. P. Lutz, B. A. Jones, P. Gambardella, A. J. Heinrich, and H. Brune, Science **344**, 988 (2014).

[6] T. Balashov, T. Schuh, A. F. Takács, A. Ernst, S. Ostanin, J. Henk, I. Mertig, P. Bruno, T. Miyamachi, S. Suga, and W. Wulfhekel, Phys. Rev. Lett. **102**, 257203 (2009).

[7] A. A. Khajetoorians, T. Schlenk, B. Schweflinghaus, M. dos Santos Dias, M. Steinbrecher, M. Bouhassoune, S. Lounis, J. Wiebe, and R. Wiesendanger, Phys. Rev. Lett. **111**, 157204 (2013).

[8] B. Bryant, A. Spinelli, J. J. T. Wagenaar, M. Gerrits, and A. F. Otte, Phys. Rev. Lett. **111**, 127203 (2013).

[9] J. M. D. Coey, *Magnetism and Magnetic Materials* (Cambridge University Press, Cambridge, UK, 2010).

[10] S. Khmelevskyi, K. Palotás, L. Szunyogh, and P. Weinberger, Phys. Rev. B **68**, 012402 (2003).

[11] C. Gould, C. Rüster, T. Jungwirth, E. Girgis, G. M. Schott, R. Giraud, K. Brunner, G. Schmidt, and L. W. Molenkamp, Phys. Rev. Lett. **93**, 117203 (2004).

[12] K. I. Bolotin, F. Kuemmeth, and D. C. Ralph, Phys. Rev. Lett. **97**, 127202 (2006).

[13] M. Viret, M. Gabureac, F. Ott, C. Fermon, C. Barreteau, G. Autes, and R. Guirado-Lopez, Eur. Phys. J. B **51**, 1 (2006).

[14] N. Néel, S. Schröder, N. Ruppelt, P. Ferriani, J. Kröger, R. Berndt, and S. Heinze, Phys. Rev. Lett. **110**, 037202 (2013).

[15] F. Strigl, C. Espy, M. Bückle, E. Scheer, and T. Pietsch, Nat. Commun. **6**, 6172 (2015).

[16] J. Schöneberg, F. Otte, N. Néel, A. Weismann, Y. Mokrousov, J. Kröger, R. Berndt, and S. Heinze, Nano Lett. **16**, 1450 (2016).

[17] M. Bode, S. Heinze, A. Kubetzka, O. Pietzsch, X. Nie, G. Bihlmayer, S. Blügel, and R. Wiesendanger, Phys. Rev. Lett. **89**, 237205 (2002).

[18] N. M. Caffrey, S. Schröder, P. Ferriani, and S. Heinze, J. Phys.: Condens. Matter **26**, 394010 (2014).

[19] I. V. Solovyev, P. H. Dederichs, and I. Mertig, Phys. Rev. B **52**, 13419 (1995).

[20] From maps and spectra of the differential conductance of the Fe layer a spurious spin polarization of the tip (e.g., from the Fe atoms at the tip) can safely be excluded.

[21] The $\pm$ values correspond to the measurement uncertainty.

[22] O. Pietzsch, A. Kubetzka, M. Bode, and R. Wiesendanger, Phys. Rev. Lett. **84**, 5212 (2000).
[23] G. Kresse and J. Furthmüller, Phys. Rev. B **54**, 11169 (1996).
[24] G. Kresse and D. Joubert, Phys. Rev. B **59**, 1758 (1999).
[25] J. P. Perdew, K. Burke, and M. Ernzerhof, Phys. Rev. Lett. **77**, 3865 (1996).
[26] S. H. Vosko, L. Wilk, and M. Nusair, Can. J. Phys. **58**, 1200 (1980).
[27] http://www.flapw.de
[28] C. Li, A. J. Freeman, H. J. F. Jansen, and C. L. Fu, Phys. Rev. B **42**, 5433 (1990).
[29] S. D. Borisova, G. G. Rusina, S. V. Eremeev, and E. V. Chulkov, JETP Lett. **103**, 471 (2016).
[30] We project the wave functions onto the atomic states in the muffin-tin spheres of the Pb atoms and discuss the orbital-decomposed LDOS in terms of p_x, p_y, and p_z states. p_y- and p_x-related features are strongly suppressed in the vacuum LDOS.
[31] K. von Bergmann, M. Menzel, D. Serrate, Y. Yoshida, S. Schröder, P. Ferriani, A. Kubetzka, R. Wiesendanger, and S. Heinze, Phys. Rev. B **86**, 134422 (2012).